Anleitung zu Versuch 23

Ferromagnetische Resonanz (FMR)

erstellt von
Dr. Thomas Meier

Fortgeschrittenenpraktikum (FOPRA)

Physik-Department
Technische Universität München

Anleitung zuletzt aktualisiert am: December 18, 2020

Contents

1 Introduction

Ferromagnetic resonance (FMR) is a widely used method for characterization of ferromagnetic samples. The magnetic moments in the sample are excited by a small alternating magnetic field with frequency in the microwave range to precess around their equilibrium position.

Using ferromagnetic resonance, the equilibrium position of the magnetization, magnetic anisotropies or dynamic properties, such as the gyromagnetic ratio or the damping of the precession of the magnetization, can be investigated. The method of ferromagnetic resonance is applicable to a wide range of magnetic samples from macroscopic samples to ultrathin layers with thicknesses in the range of single atomic layers or even to nanostructured magnetic devices.

Because of these properties, FMR has also gained great importance in research for modern computer technology. Computer technology in its current form is limited in its development towards ever more densely packed and smaller transistors by the ohmic heat loss in the transistors, which leads to an ever increasing heating of the components due to the decreasing size of the transistors. This problem is to be solved in the future by replacing charge currents by spin currents in so-called spintronic devices. In these devices, information will no longer be transported by charge but by spin orientation, so that ohmic losses no longer occur. FMR can be used to characterize the respective samples or to generate spin currents to test spin effects, such as the spin Hall effect.

Ferromagnetic resonance was first experimentally discovered independently by J. Griffiths and E. Zavoisky in 1919. Zavoisky in 1946 [1, 2], ,after it was observed by chance already in 1911 by V. K. Arkad'yev. The first theoretical description was given by C. Kittel in 1948 [3]. The underlying problem of the relaxation dynamics of the magnetization vector had already been theoretically treated by Landau and Lifshitz in 1935, which finally led to the development of the basic equation of magnetization dynamics, the so-called Landau-Lifshitz-Gilbert equation (LLG). [4, 5].

Exercise 1: Read the following introduction to the theory of FMR and to the experimental setup thoroughly and try to understand all essential aspects before performing the experiment. Also work on the other tasks contained in the following text.

2 Theoretical Basics

In this section the basic theoretical aspects of ferromagnetic resonance shall be made understandable. It starts with a very short introduction to the ferromagnetism of 3d transition metals and the introduction of the main energy contributions in the ferromagnet. In the following the Landau-Lifshitz-Gilbert equation is discussed and the derivation of the resonance condition is explained. Finally, a phenomenological description of the damping effects in ferromagnets observed in experiments is briefly presented. The whole chapter follows in large parts [6].

2.1 Ferromagnetism - a brief introduction

Few subjects in science are more difficult to understand than magnetism.
Encyclopedia Brittanica, 1989

What is already true for magnetism in general is especially true for ferromagnetism, since it is one of the most important everyday phenomena that can no longer be described by classical physics. The exchange interaction underlying ferromagnetism, which leads to a spontaneous parallel alignment of the magnetic moments in the ferromagnet, is a purely quantum mechanical phenomenon, which results from the interaction of the Coulomb repulsion of the electrons with the Pauli principle.

The ferromagnetism of the so-called 3d transition metals iron, cobalt and nickel is particularly complex, since the magnetic moments are represented by electrons in 3d states, which are partially delocalized, i.e. can move almost freely through the crystal lattice. Since the exact explanation by means of band structure models would require extensive knowledge of solid state physics, a simpler illustrative explanation shall be presented here.

Based on the Pauli principle of quantum mechanics, electrons with the same spin must not be located at the same place, since they would then coincide in all quantum numbers. The closer two electrons are to each other, the greater their Coulomb energy becomes because of the repulsion of their equal charges. If we now assume that the electrons have the same spin state, the Pauli principle forbids that the electrons are in the same place. Therefore, for electrons with parallel spin, the average distance between the electrons increases and the Coulomb energy is minimized. According to this consideration, it would be advantageous for all metals to spontaneously form parallel spins, i.e. ferromagnetism. So there must still be an opposite effect, which energetically disadvantages the parallel alignment of the spins. This can also be explained by the Pauli principle. If the electrons have parallel spin, then according to the Pauli principle, the impulses of the electrons must not coincide, because otherwise the electrons would be equal in all quantum numbers. Since the states with low momentum are already all occupied, states with higher momentum than before must be occupied during the transition from opposite to parallel spins, so that the average kinetic energy of the electrons increases. Paragraph based on [7–9].

For most metals, the increase in kinetic energy exceeds the reduction in Coulomb energy, so that no spontaneous parallel arrangement of spins, i.e., no ferromagnetism, results. Only for very few materials is the parallel arrangement of spins more favorable, such as iron, cobalt and nickel. These materials become ferromagnetic below a characteristic temperature, the Curie temperature T_C , and show a spontaneous parallel alignment of neighboring spins [8, 9].

2.2 Magnetic Energy and Anisotropy

In this section the most important energy contributions in ferromagnetic samples are explained. For the samples considered in this practical experiment, the so-called macrospin approximation shall be applied. This assumes that all magnetic moments in the sample are aligned in parallel due to the exchange interaction, and that the magnetic state of the sample can therefore be described by a single magnetization vector [10, 11]. In general, this approximation is only suitable for thin samples that are uniformly magnetized in the sample plane.

The first energy contribution in the ferromagnet is the exchange energy, which is larger the more the magnetic moments deviate from the parallel alignment. Since the macrospin approximation is used here, where all moments are always parallel, the exchange energy is constant and need not be considered further.

2.2.1 Demagnetizing Energy

The first energy contribution relevant for the experiment is the demagnetizing energy. This can be considered as a direct consequence of Maxwell's equations in a spontaneously magnetized body.As should already be known from the lectures on electrodynamics, two magnetic field quantities are needed to describe a ferromagnetic material. One is the magnetic induction $\vec{B}$, the other is the magnetic field $\vec{H}$. These two field quantities are related to the magnetization by a simple equation [8]:

$$\vec{B} = \mu_0 \left(\vec{H} + \vec{M} \right) \tag{1}$$

In this tutorial, SI units will be used instead of the cgs units still commonly used in FMR theory. The unit for the magnetic induction is therefore $[B] = 1$ T (Tesla) and for the magnetic field is $[H] = 1 \ \frac{\mathrm{A}}{\mathrm{m}}$.

Furthermore, for the B-field the following Maxwell equations are valid:

$$\vec{\nabla} \cdot \vec{B} = 0 \tag{2}$$

The magnetic field $\vec{H}$ is unlike the magnetic induction $\vec{B}$ non-source-free. Substituting equation (1) into equation (2) gives thedivergence of $\vec{H}$, which in general does not vanish.

$$\vec{\nabla} \cdot \vec{H} = -\vec{\nabla} \cdot \vec{M} \tag{3}$$

The $\vec{H}$-field can be decomposed into a sum of two fields [8].

$$\vec{H} = \vec{H}_{\mathrm{ex}} + \vec{H}_{\mathrm{d}} \tag{4}$$

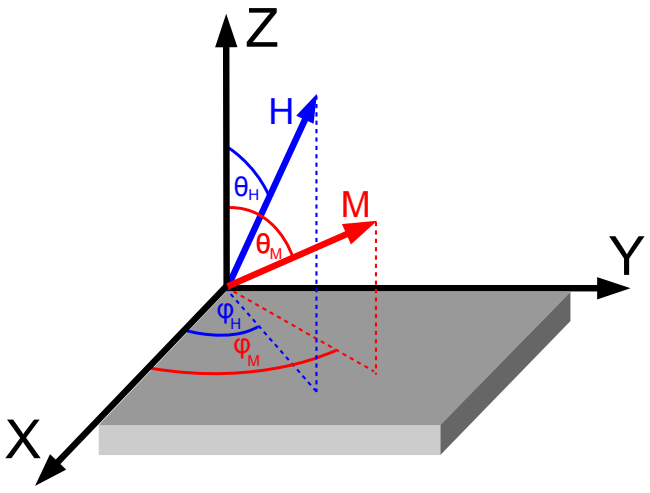

Figure 1: The figure shows the coordinate system XYZ of the sample, which is used in the calculations of the demagnetizing field of a thin film and in the calculation of energy densities. The angles describing the magnetization $\vec{M}$ and the magnetic field $\vec{H}$ are also shown in the graph.

The first part is the external field $\vec{H}_{ex}$ caused by currents or other magnets, the second part $\vec{H}_d$ is called demagnetizing field inside the sample and stray field outside the sample [8].

The decomposition is chosen in such a way that the demagnetizing field is a conservative field and can therefore be represented as a gradient of a potential generated by so-called magnetic charges. Analogous to the first Maxwell's equation for the electric field $\vec{\nabla} \cdot \vec{E} = \frac{\rho}{\epsilon_0}$ with the charge density ρ the density of the magnetic charges may be identified by comparison with equation 3 [8].

$$\rho_{\mathrm{m}} = -\vec{\nabla} \cdot \vec{M} \tag{5}$$

In a homogeneously magnetized sample, the magnetic charges are therefore located on the interface, since the magnetization changes there ($\vec{\nabla} \cdot \vec{M} \neq 0$). The demagnetizing field acts in the opposite direction to the magnetization, which explains the name [10].

For ellipsoidal homogeneously magnetized samples, the demagnetizing field can be calculated exactly. It turns out that the demagnetizing field is linearly related to the magnetization and therefore also homogeneous [8, 11].

$$\vec{H}_{\mathrm{d}} = -\mathcal{N}\vec{M}, \tag{6}$$

with the demagnetization tensor $\mathcal{N}$, where the trace of the demagnetization tensor $\mathrm{Tr}(\mathcal{N}) = 1$ [8].

For a thin, widely extended film, the length and width are much larger than the thickness. Therefore, the components of the demagnetizing field parallel to the surface (X and Y directions) can be neglected since the magnetic charges are very far apart [10, 12]. This corresponds to $\mathcal{N}_{XX}= 0$ and $\mathcal{N}_{YY}= 0$. Since the trace of the demagnetization tensor is one, $\mathcal{N}_{ZZ}= 1$ must apply.

The demagnetizing energy is now the energy of a ferromagnetic sample in its own demagnetizing field. For a change of the magnetization by $d\vec{M}$ in any magnetic field $\vec{H}$, the change of the energy density is:

$$\mathrm{d}\epsilon = -\mu_0 \vec{H} \cdot \mathrm{d}\vec{M} \tag{7}$$

To calculate the demagnetization energy density, the demagnetizing field from equation(6) is substituted into the last equation in place of $\vec{H}$. The magnetization vector is then split into magnitude and direction, so that $\vec{M} = M\vec{m}$ applies with the magnitude of the magnetization M and the unit direction vector $\vec{m}$. For a sample magnetized to saturation,the above equation must be integrated from 0 to the saturation magnetization M_S in M and the expression follows

$$\epsilon_\mathrm{dem} = \frac{1}{2}\mu_0 M_\mathrm{S}^2 \; \vec{m}(\mathcal{N}\vec{m}) \tag{8}$$

Exercise 2: Follow exactly the derivation given in the previous section and calculate the demagnetization energy density of a thin film as a function of the angle θ_M (see Fig. 1).Which equilibrium orientation of the magnetization is preferred by the demagnetizing energy in a thin film?

2.2.2 Magnetocristalline Anisotropy

Magnetocrystalline anisotropy means that in a ferromagnetic body certain directions of magnetization are energetically preferred [12]. The preferred directions are determined by the symmetry and structure of the crystal lattice [8, 10, 12]. The physical cause of the anisotropy lies in the spin-orbit interaction. The spin-orbit interaction couples the orbital motion of electrons with their spin [8, 12].

While the permalloy samples studied in this experiment should not exhibit anisotropies due to the specially tuned composition of this Ni/Fe alloy, the occurrence of such magnetocrystalline anisotropies is typical mainly for epitaxially grown crystalline films. The simplest form of anisotropy is a uniaxial anisotropy pointing out of the sample plane, described by the following formula

$$\epsilon_\mathrm{ani} = -K_\mathrm{U}^{\perp} m_\mathrm{Z}^2 \; . \tag{9}$$

Where $K_\mathrm{U}^{\perp}$ is the associated anisotropy constant (Unit: $\frac{\mathrm{J}}{\mathrm{m}^3}$) and m_Z is the Z-component of the unit magnetization vector (see Fig. 1 for the coordinate system). This type of anisotropy often occurs due to interfacial effects or strain in ultrathin films and can become so strong that the equilibrium position of the magnetization is perpendicular to the sample plane.

2.2.3 Zeeman Energy

If a magnetized sample is in an external magnetic field Hexso the magnetic moments of the sample interact with the external field and theparallel alignment of the magnetization and the external field is more energetically favorable. The corresponding term in the energy density is called Zeeman term and is:

$$\epsilon_{\mathrm{zee}} = -\mu_0 M_{\mathrm{S}} \vec{H}_{\mathrm{ex}} \cdot \vec{m} \tag{10}$$

2.2.4 Total energy density and effective field

The total energy density is calculated as the sum of demagnetization, anisotropy and Zeeman energy density

$$\epsilon = \frac{1}{2}\mu_0 M_{\mathrm{S}}^2 m_{\mathrm{Z}}^2 - K_{\mathrm{U}}^{\perp} m_{\mathrm{Z}}^2 - \mu_0 M_{\mathrm{S}} \vec{H}_{\mathrm{ex}} \cdot \vec{m} \tag{11}$$

For further theoretical considerations the effective magnetic field $\vec{H}_{\mathrm{EFF}}$ is of great importance. It is calculated by forming the gradient of the total energy density with respect to the coordinates of the magnetization $\vec{M}$ [10, 12, 13].

$$\mu_0 \vec{H}_{\mathrm{EFF}} = -\frac{1}{M_{\mathrm{S}}} \vec{\nabla}_{\vec{m}}\, \epsilon \tag{12}$$

Exercise 3: Calculate the effective field.

2.2.5 Finding the equilibrium position of the magnetization

The equilibrium position of the magnetization is given by a minimum of thetotal energy density in equation (11) **under the constraint that theamount of the unit magnetization vector is 1.** For this purpose, it is convenient to parameterize $\vec{m}$ and the external magnetic field $\vec{H}_{\mathrm{ex}}$ in spherical coordinates according to 1. Then, derive according to the angles θ_{M} and φ_{M} and set both derivatives to zero.

Exercise 4: Determine the equilibrium position of the magnetization according to the above instructions.

At the end, you should get the following result:

$$M_{\mathrm{eff}} \cos(\theta_{\mathrm{M}}) \sin(\theta_{\mathrm{M}}) + H_0 \sin(\theta_{\mathrm{H}} - \theta_{\mathrm{M}}) = 0 \tag{13}$$

$$\varphi_{\mathrm{H}} = \varphi_{\mathrm{M}}\ , \tag{14}$$

where H_0 is the magnitude of the external magnetic field and the effective magnetization $M_{\mathrm{eff}} = M_{\mathrm{S}} - \frac{2K_U^{\perp}}{\mu_0 M_{\mathrm{S}}}$ is introduced.

It is important to understand that in a ferromagnetic sample, due to anisotropies, the directions of magnetization and external magnetic field are generally **not parallel**.

2.3 Landau-Lifshitz-Gilbert equation

After always assuming a constant magnetization in time in the previous considerations, the time evolution of the magnetization vector shall now be investigated. If, for example, the magnetization of a thin film is deflected from its equilibrium position by an external field, then a precession of the magnetization around the effective magnetic field can be observed. In this process, the magnetization returns on a spiral path to its equilibrium position, where it is parallel to the effective magnetic field. The time scale for this process is in the nanosecond range [10, 12]. This behavior of magnetization was already described theoretically by Landau and Lifschitz in 1935 by the Landau-Lifschitz equation [4].

The first part of the Landau-Lifschitz equation describes the precession of the magnetization around the effective magnetic field[4, 10].

$$\frac{\mathrm{d}\vec{M}}{\mathrm{d}t} = -\gamma\mu_0 \, \vec{M} \times \vec{H}_{\mathrm{eff}} \tag{15}$$

Here $\gamma = \frac{eg}{2m_\mathrm{e}}$ designates the gyromagnetic relation of the electron with the elementary charge, the electron mass and the g-factoror; g, which is used for free electrons is approximately $2,0023$. This equation describes in general an elliptic precession of the magnetization around the effective magnetic field.

However, the above equation cannot yet describe that the magnetization returns to the equilibrium position, a damping mechanism is missing. Already Landau and Lifschitz inserted a damping term into their equation [4]. However, since this term gives a physically incorrect behavior for large dampings, Gilbert introduced an improved damping term in 1955 which gives the correct physical behavior [5, 10]. By adding this damping term to equation (15), the Landau-Lifschitz-Gilbert equation (LLG) is obtained. [10, 12]

$$\frac{\mathrm{d}\vec{m}}{\mathrm{d}t} = -\gamma\mu_0 \, \vec{m} \times \vec{H}_{\mathrm{eff}} + \alpha \, \vec{m} \times \frac{\mathrm{d}\vec{m}}{\mathrm{d}t} \tag{16}$$

Here, the unit magnetization vector $\vec{m} = \vec{M}/M_\mathrm{S}$ was used and the Gilbert damping parameter α was introduced, which indicates the strength of the damping.The second term of the sum is called the Gilbert damping term and leads to the Relaxation of the magnetization to the equilibrium position[10]. Figure 2 shows a numerical solution of the LLG. Under the influence of the LLG, the magnetization basically moves on a spherical surface. [12].

Exercise 5: Consider the direction in which the individual contributions to the LLG point. Justify mathematically and graphically why the magnetization must always move on a spherical surface.

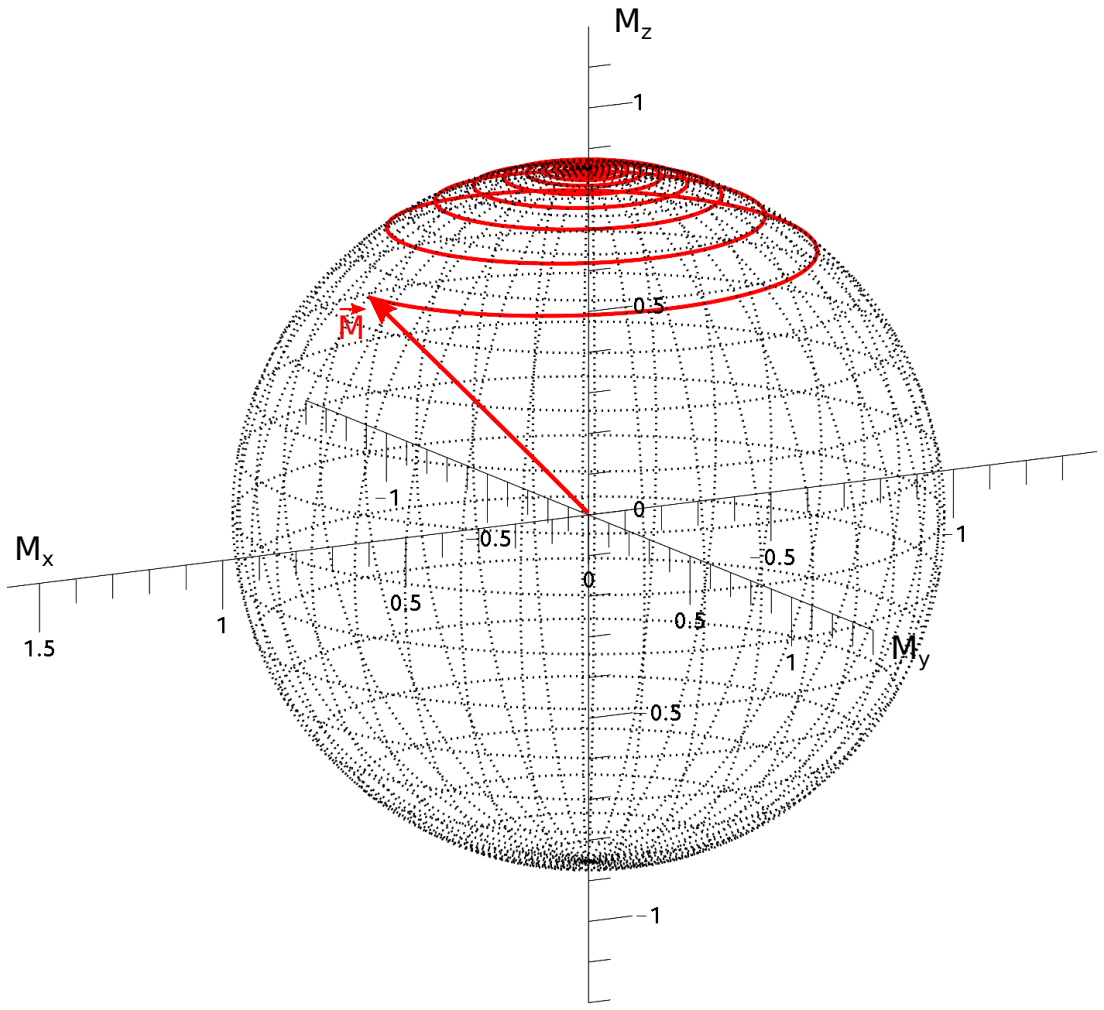

Figure 2: Numerical solution of the Landau-Lifschitz-Gilbert equation for $\gamma = 200\ \frac{\text{GHz}}{\text{T}}$, $\alpha = 0,05$ und $\mu_0 M_S = 0,852$ T. Note tha a very high attenuation was chosen for better visualization has been chosen. The effective field points in the z-direction with a constant strength of 1 T. You can see the spiral precession of the magnetization towards the equilibrium position in z-direction (red line). In addition, a spherical surface is indicated by the black dotted lines.

2.4 Ferromagnetic resonance - resonance condition

2.4.1 Principles of FMR

As already indicated in the introduction, measurements of ferromagnetic resonance can be used to determine certain properties of magnetic materials, such as the g-factor or the Gilbert damping parameter α or the magnetic anisotropies [12, 13].

In an FMR experiment, the precession of the magnetization is excited with a high-frequency magnetic field in the microwave range. The sample is in an external time-independent magnetic field $\vec{H}_0$.The precession of the magnetization around the effective field absorbs energy from the microwave field. Ferromagnetic resonance occurs at a fixed microwave angular frequency ω in a certain external magnetic field H_{FMR} and is detected by a maximum of microwave absorption. The evaluation of FMR measurements focuses on the resonance position and the line width of the measured resonance curve.

2.4.2 Definition of a suitable coordinate system

In order to simplify the calculation of the resonance condition in the following subchapters, a suitable coordinate system is to be introduced. As in the previous chapters, XYZ is the coordinate system whose z-axis is normal to the sample plane. Similarly, the angle θ_M of the magnetization with respect to the Z-axis and the angle φ_M between the projection of the magnetization in the X-Y plane and the X-axis are again used.For the calculation of the resonance condition of FMR, the coordinate system XYZ is not convenient and therefore the coordinate systemxyz is used in the following with its x-axis pointing in the direction of $\vec{M}$. In Fig. 3 , the two coordinate systems and the magnetization vector are shown.

The coordinate transformation from the system XYZ into the system xyz, with which a vector in the system XYZ can be transferred into the system xyz, is given by the following equation

$$\begin{aligned}\begin{pmatrix} M_x \\ M_y \\ M_z \end{pmatrix} &= T_{XYZ}^{xyz} \begin{pmatrix} M_X \\ M_Y \\ M_Z \end{pmatrix} = \\ &= \begin{pmatrix} \sin\theta_M \cos\varphi_M & \sin\theta_M \sin\varphi_M & \cos\theta_M \\ -\sin\varphi_M & \cos\varphi_M & 0 \\ -\cos\theta_M \cos\varphi_M & -\cos\theta_M \sin\varphi_M & \sin\theta_M \end{pmatrix} \begin{pmatrix} M_X \\ M_Y \\ M_Z \end{pmatrix}\end{aligned} \tag{17}$$

The following calculations also require the transformation from system xyz to

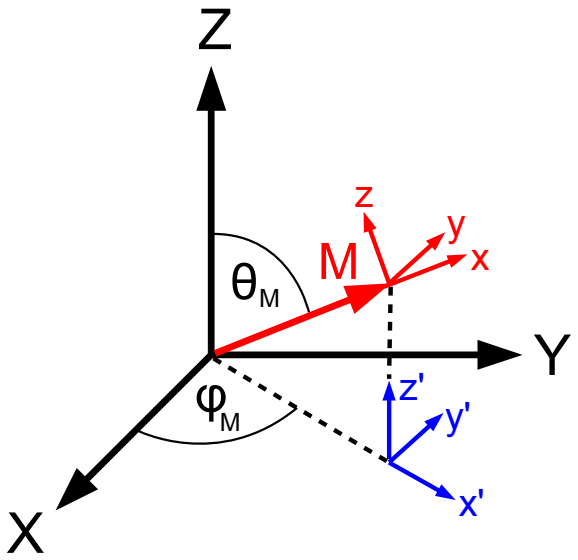

Figure 3: In dieser Abbildung sind die beiden für die weiteren Berechnungen benötigten Koordinatensysteme, ein Hilfskoordinatensystem und der Magnetisierungsvektor dargestellt.

system XYZ. This is given by

$$\begin{pmatrix} M_X \\ M_Y \\ M_Z \end{pmatrix} = T_{xyz}^{XYZ} \begin{pmatrix} M_x \\ M_y \\ M_z \end{pmatrix} = \tag{18}$$

$$= \begin{pmatrix} \sin\theta_M \cos\varphi_M & -\sin\varphi_M & -\cos\theta_M \cos\varphi_M \\ \sin\theta_M \sin\varphi_M & \cos\varphi_M & -\cos\theta_M \sin\varphi_M \\ \cos\theta_M & 0 & \sin\theta_M \end{pmatrix} \begin{pmatrix} M_x \\ M_y \\ M_z \end{pmatrix} .$$

Exercise 6: Based on your knowledge of linear algebra, work out how these two transformation matrices come about. You do not have to calculate the transfer matrices exactly.

2.4.3 Calculation of the effective field

The effective field, which you have already calculated in a preparatory task in the coordinate system XYZ, must now be transferred to the coordinate system xyz relevant for the FMR. This is done by multiplication with the transfer matrix in

equatio 17, so that $\mu_0\vec{H}_{\mathrm{eff}} = T^{xyz}_{XYZ}\ (\mu_0\vec{H}_{\mathrm{EFF}})$. This gives:

$$\begin{aligned}
\mu_0 H_{\mathrm{eff,x}} =& \mu_0 \sin(\theta_{\mathrm{M}}) \cos(\varphi_{\mathrm{M}}) H_{\mathrm{ex,X}} + \mu_0 \sin(\theta_{\mathrm{M}}) \sin(\varphi_{\mathrm{M}}) H_{\mathrm{ex,Y}} + \\
& \mu_0 \cos(\theta_{\mathrm{M}}) H_{\mathrm{ex,Z}} - \mu_0 \cos(\theta_{\mathrm{M}}) M_{\mathrm{eff}} m_{\mathrm{Z}} && (19)\\
\mu_0 H_{\mathrm{eff,y}} =& -\mu_0 \sin(\varphi_{\mathrm{M}}) H_{\mathrm{ex,X}} + \mu_0 \cos(\varphi_{\mathrm{M}}) H_{\mathrm{ex,Y}} && (20)\\
\mu_0 H_{\mathrm{eff,z}} =& -\mu_0 \cos(\theta_{\mathrm{M}}) \cos(\varphi_{\mathrm{M}}) H_{\mathrm{ex,X}} - \mu_0 \cos(\theta_{\mathrm{M}}) \sin(\varphi_{\mathrm{M}}) H_{\mathrm{ex,Y}} + \\
& \mu_0 \sin(\theta_{\mathrm{M}}) H_{\mathrm{ex,Z}} - \mu_0 \sin(\theta_{\mathrm{M}}) M_{\mathrm{eff}} m_{\mathrm{Z}} && (21)
\end{aligned}$$

Now the magnetization components Z must be replaced by the magnetization components in the coordinate system xyz. This is done by using the back transformation T^{XYZ}_{xyz} from equation(18), so that

$$m_{\mathrm{Z}} = \cos(\theta_{\mathrm{M}}) m_{\mathrm{x}} + \sin(\theta_{\mathrm{M}}) m_{\mathrm{z}} \tag{22}$$

is valid. Furthermore, the static external field $\vec{H}_0$ is to be expressed by spherical coordinates and a small microwave excitation field h has to be added with the angular frequency ω.

$$\vec{H}_{\mathrm{ex}} = \begin{pmatrix} H_0 \sin(\theta_{\mathrm{H}}) \cos(\varphi_{\mathrm{H}}) \\ H_0 \sin(\theta_{\mathrm{H}}) \sin(\varphi_{\mathrm{H}}) \\ H_0 \cos(\theta_{\mathrm{H}}) \end{pmatrix} + \vec{h} \exp(i\omega t) \tag{23}$$

Using the addition theorems for the trigonometric functions, the effective field can be calculated from equations (22) and (23) simplifying the following expression

$$\begin{aligned}
\mu_0 H_{\mathrm{eff,x}} =& \mu_0 H_0 \left(\sin(\theta_{\mathrm{M}}) \sin(\theta_{\mathrm{H}}) \cos(\varphi_{\mathrm{H}} - \varphi_{\mathrm{M}}) + \cos(\theta_{\mathrm{M}}) \cos(\theta_{\mathrm{H}})\right) - \\
& \mu_0 M_{\mathrm{eff}} \cos(\theta_{\mathrm{M}}) \left(\cos(\theta_{\mathrm{M}}) m_{\mathrm{x}} + \sin(\theta_{\mathrm{M}}) m_{\mathrm{z}}\right) + \mu_0 h_{\mathrm{x}} \exp(i\omega t) && (24)\\
\mu_0 H_{\mathrm{eff,y}} =& \mu_0 H_0 \sin(\theta_{\mathrm{M}}) \sin(\varphi_{\mathrm{H}} - \varphi_{\mathrm{M}}) + \mu_0 h_{\mathrm{y}} \exp(i\omega t) && (25)\\
\mu_0 H_{\mathrm{eff,z}} =& \mu_0 H_0 \left(-\cos(\theta_{\mathrm{M}}) \sin(\theta_{\mathrm{H}}) \cos(\varphi_{\mathrm{H}} - \varphi_{\mathrm{M}}) + \sin(\theta_{\mathrm{M}}) \cos(\theta_{\mathrm{H}})\right) - \\
& \mu_0 M_{\mathrm{eff}} \sin(\theta_{\mathrm{M}}) \left(\cos(\theta_{\mathrm{M}}) m_{\mathrm{x}} + \sin(\theta_{\mathrm{M}}) m_{\mathrm{z}}\right) + \mu_0 h_{\mathrm{z}} \exp(i\omega t) && (26)
\end{aligned}$$

In FMR experiments, the microwave excitation is usually so small that the magnetization is never strongly deflected from its equilibrium position (i.e. mx $\approx$1 and my,mz $\ll 1$), so using the equilibrium position of the magnetization found in section2.2.5, the effective field can be further simplified [10].

$$\begin{aligned}
\mu_0 H_{\mathrm{eff,x}} =& \mu_0 H_0 \cos(\theta_{\mathrm{H}} - \theta_{\mathrm{M}}) - \mu_0 M_{\mathrm{eff}} \cos(\theta_{\mathrm{M}}) \Big(\cos(\theta_{\mathrm{M}}) m_{\mathrm{x}} + \\
& \sin(\theta_{\mathrm{M}}) m_{\mathrm{z}} \Big) + \mu_0 h_{\mathrm{x}} \exp(i\omega t) && (27)\\
\mu_0 H_{\mathrm{eff,y}} =& \mu_0 h_{\mathrm{y}} \exp(i\omega t) && (28)\\
\mu_0 H_{\mathrm{eff,z}} =& -\mu_0 M_{\mathrm{eff}} \sin^2(\theta_{\mathrm{M}}) m_{\mathrm{z}} + \mu_0 h_{\mathrm{z}} \exp(i\omega t) && (29)
\end{aligned}$$

2.4.4 Solution of the linearized LLG

The driven motion of the magnetization vector under a high frequency magnetic field is described by the Landau-Lifshitz-Gilbert equation. Since this is a nonlinear differential equation, an analytical solution is generally not possible. However, for small excitation fields $\vec{h}$ a linearization according to the following approach for the unit magnetization vector is possible.

$$\vec{m} = \begin{pmatrix} 1 \\ \mathfrak{m}_\mathrm{y} \exp(i\omega t) \\ \mathfrak{m}_\mathrm{z} \exp(i\omega t) \end{pmatrix} \tag{30}$$

Exercise 7: Substitute the approximation from equation (??) into the LLG (16) and simplify as much as possible (without using the effective field explicitly). Linearize the obtained equations for all components as much as possible (i.e., neglect quadratic orders in $\mathfrak{m}_\mathrm{y}$ and $\mathfrak{m}_\mathrm{z}$).

The effective field from equations (27) to (29) is now substituted into the result you calculated and again all quadratic orders in $\mathfrak{m}_\mathrm{y}$ and $\mathfrak{m}_\mathrm{z}$ are neglected. Furthermore, due to the small microwave excitation field, mixing terms between the components of $\vec{h}$ and $\mathfrak{m}_\mathrm{y}$ and $\mathfrak{m}_\mathrm{z}$ can also be neglected. With these simplifications, the x-component of the LLG becomes trivial and we are left with the following two equations [10, 12, 13]:

$$0 = i\frac{\omega}{\gamma}\mathfrak{m}_\mathrm{y} + \left(\mathfrak{B}_\mathrm{eff} + \alpha i\frac{\omega}{\gamma}\right)\mathfrak{m}_\mathrm{z} - \mu_0 h_\mathrm{z} \tag{31}$$

$$0 = -i\frac{\omega}{\gamma}\mathfrak{m}_\mathrm{z} + \left(\mu_0\mathfrak{H}_\mathrm{eff} + \alpha i\frac{\omega}{\gamma}\right)\mathfrak{m}_\mathrm{y} - \mu_0 h_\mathrm{y} \tag{32}$$

Here, the effective magnetic induction $\mathfrak{B}_\mathrm{eff}$ and the effective magnetic field $\mathfrak{H}_\mathrm{eff}$ were introduced, so that [10, 12, 13]

$$\mathfrak{B}_\mathrm{eff} = \mu_0 H_0 \cos(\theta_\mathrm{H} - \theta_\mathrm{M}) - \mu_0 M_\mathrm{eff} \cos(2\theta_\mathrm{M}) \tag{33}$$

$$\mu_0\mathfrak{H}_\mathrm{eff} = \mu_0 H_0 \cos(\theta_\mathrm{H} - \theta_\mathrm{M}) - \mu_0 M_\mathrm{eff} \cos^2(\theta_\mathrm{M})\ . \tag{34}$$

Exercise 8: Solve the system of linear equations for $\mathfrak{m}_\mathrm{y}$ and $\mathfrak{m}_\mathrm{z}$.

2.4.5 Resonance condition

The resonance condition of the FMR can be read from the results for $\mathfrak{m}_\mathrm{y}$ and $\mathfrak{m}_\mathrm{z}$. Neglecting the usually very small damping α, the maximum of the precession amplitude of the magnetization is given by the zero of the denominator of $\mathfrak{m}_\mathrm{y}$ or $\mathfrak{m}_\mathrm{z}$. This generally leads to the following resonance condition, which specifies

the microwave angular frequency for which resonance occurs at a given magnetic field H_{FMR} [10, 12, 13]:

$$\left(\frac{\omega}{\gamma}\right)^2 = \mu_0 \mathfrak{B}_{\mathrm{eff}} \mathfrak{H}_{\mathrm{eff}} \Big|_{H_0 = H_{\mathrm{FMR}}} \tag{35}$$

The two most important special cases are discussed below:

2.4.5.1 In-plane configuration In the in-plane configuration, both the external field and the magnetization lie in the sample plane ($\theta_{\mathrm{H}} = 90°$ and $\theta_{\mathrm{M}} = 90°$) and are parallel ($\varphi_{\mathrm{H}} = \varphi_{\mathrm{M}}$). There must be no in-plane anisotropies in the sample. By substituting these angles into equation (33) and (34), the following resonance condition is found, also known as the Kittel formula due to its discovery by C. Kittel in 1948 [3]:

$$\frac{\omega}{\gamma} = \sqrt{\mu_0 H_{\mathrm{FMR}} (\mu_0 H_{\mathrm{FMR}} + \mu_0 M_{\mathrm{eff}})} \tag{36}$$

2.4.5.2 Out-of-plane configuration Here, the applied magnetic field is perpendicular to the sample plane $\theta_{\mathrm{H}} = 0°$. It is assumed that magnetization and external field are parallel in this process. For in-plane magnetized samples this is ensured by applying a very high external field in which the sample is saturated, for out-of-plane magnetized samples the assumption is always fulfilled. By setting the angles in equation (33) and (34) to zero the following resonance condition is obtained:

$$\frac{\omega}{\gamma} = \mu_0 H_{\mathrm{FMR}} - \mu_0 M_{\mathrm{eff}} \tag{37}$$

Exercise 9: Verify the resonance conditions presented here using your results for $\mathfrak{m}_{\mathrm{y}}$ and $\mathfrak{m}_{\mathrm{z}}$.

2.4.6 Dynamic susceptibilities and line shape of the FMR

While in the last subchapter the position of the ferromagnetic resonance was derived, now the shape of the absorption curves measured in the experiment shall be derived. First of all, the dynamic susceptibilities are defined by

$$\vec{\mathfrak{m}} = \chi \vec{h} \tag{38}$$

with the susceptibility tensor χ.

Using the results for $\mathfrak{m}_{\mathrm{y}}$ and $\mathfrak{m}_{\mathrm{z}}$ from the previous subsection, the components

of the susceptibility tensor can be determined.

$$\chi_{yy} = \frac{-\mu_0 \left(\mathfrak{B}_{\text{eff}} + \frac{i\alpha\omega}{\gamma}\right)}{\left(\frac{\omega}{\gamma}\right)^2 - \left(\mathfrak{B}_{\text{eff}} + \frac{i\alpha\omega}{\gamma}\right)\left(\mu_0\mathfrak{H}_{\text{eff}} + \frac{i\alpha\omega}{\gamma}\right)} \tag{39}$$

$$\chi_{yz} = -\chi_{zy} = \frac{-\mu_0 \frac{i\omega}{\gamma}}{\left(\frac{\omega}{\gamma}\right)^2 - \left(\mathfrak{B}_{\text{eff}} + \frac{i\alpha\omega}{\gamma}\right)\left(\mu_{\text{eff}}\mathfrak{H}_{\text{eff}} + \frac{i\alpha\omega}{\gamma}\right)} \tag{40}$$

$$\chi_{zz} = \frac{-\mu_0 \left(\mathfrak{H}_{\text{eff}} + \frac{i\alpha\omega}{\gamma}\right)}{\left(\frac{\omega}{\gamma}\right)^2 - \left(\mathfrak{B}_{\text{eff}} + \frac{i\alpha\omega}{\gamma}\right)\left(\mu_0\mathfrak{H}_{\text{eff}} + \frac{i\alpha\omega}{\gamma}\right)} \tag{41}$$

The microwave absorption in the sample and the measured line shape is given by the imaginary part of the susceptibilities. In the following, the line shape of χ_{yy} is derived as an example. The calculations can be carried out for the other susceptibilities in an analogous way.

Equation (39) for χ_{yy} is assumed. For $\left(\frac{\omega}{\gamma}\right)^2$ the resonance condition from equation (35) is used. Then the numerator and denominator are developed around the resonant field H_{FMR} in H_0 to linear order and terms proportional to $\alpha(H_0 - H_{\text{FMR}})$ or α^2 are neglected. This yields:

$$\chi_{yy} = \frac{\mu_0 \left(\mathfrak{B}_{\text{FMR}} + \frac{\partial\mathfrak{B}_{\text{eff}}}{\partial H_0}\Big|_{H_0=H_{\text{FMR}}} \delta H + i\mu_0\Delta H\right)}{\left(\mathfrak{B}_{\text{FMR}}\frac{\partial\mathfrak{H}_{\text{eff}}}{\partial H_0}\Big|_{H_0=H_{\text{FMR}}} + \mathfrak{H}_{\text{FMR}}\frac{\partial\mathfrak{B}_{\text{eff}}}{\partial H_0}\Big|_{H_0=H_{\text{FMR}}}\right)\mu_0\delta H + (\mathfrak{B}_{\text{FMR}} + \mu_0\mathfrak{H}_{\text{FMR}})i\mu_0\Delta H)} \tag{42}$$

Here, the effective field and the effective magnetization in the resonance case, $\mathfrak{H}_{\text{FMR}} = \mathfrak{H}_{\text{eff}}\Big|_{H_0=H_{\text{FMR}}}$ and $\mathfrak{B}_{\text{FMR}} = \mathfrak{B}_{\text{eff}}\Big|_{H_0=H_{\text{FMR}}}$.$\delta H$ is the difference between external field and resonant field $H_0 - H_{\text{FMR}}$. In addition, the linewidth (half width at half maximum) was defined as $\mu_0\delta H = \frac{\alpha\omega}{\gamma}$.

By calculating the derivatives using equations (34) and (33) and multiplying by the complex conjugate of the denominator, the line shape of the susceptibility χ_{yy} is obtained.

$$\chi_{yy} = \frac{\mathfrak{B}_{\text{FMR}}}{(\mathfrak{B}_{\text{FMR}} + \mu_0\mathfrak{H}_{\text{FMR}})\Delta H}\left(\frac{\Delta H(H_0 - H_{\text{FMR}}) - i\Delta H^2}{(H_0 - H_{\text{FMR}})^2 + \Delta H^2} + \frac{\mu_0\Delta H}{\mathfrak{B}_{\text{FMR}}}\right) \tag{43}$$

Thus, it can be seen that the real part of the susceptibility χ_{yy} has the shape of an antisymmetric Lorentz curve, while the imaginary part has the shape of a symmetric Lorentz curve. The line shape of all susceptibilities is exemplarily shown in figure 4.

It can be shown that the microwave power absorbed by the sample is determined by the imaginary parts of χ_{yy} and χ_{zz}. Therefore, FMR resonance curves have the form of symmetric Lorentz curves. For the mean absorbed power, [12, 14] holds:

$$\bar{P} = \frac{1}{2}\mu_0 M_S\omega\left(\Im(\chi_{yy})h_y^2 + \Im(\chi_{zz})h_z^2\right) \tag{44}$$

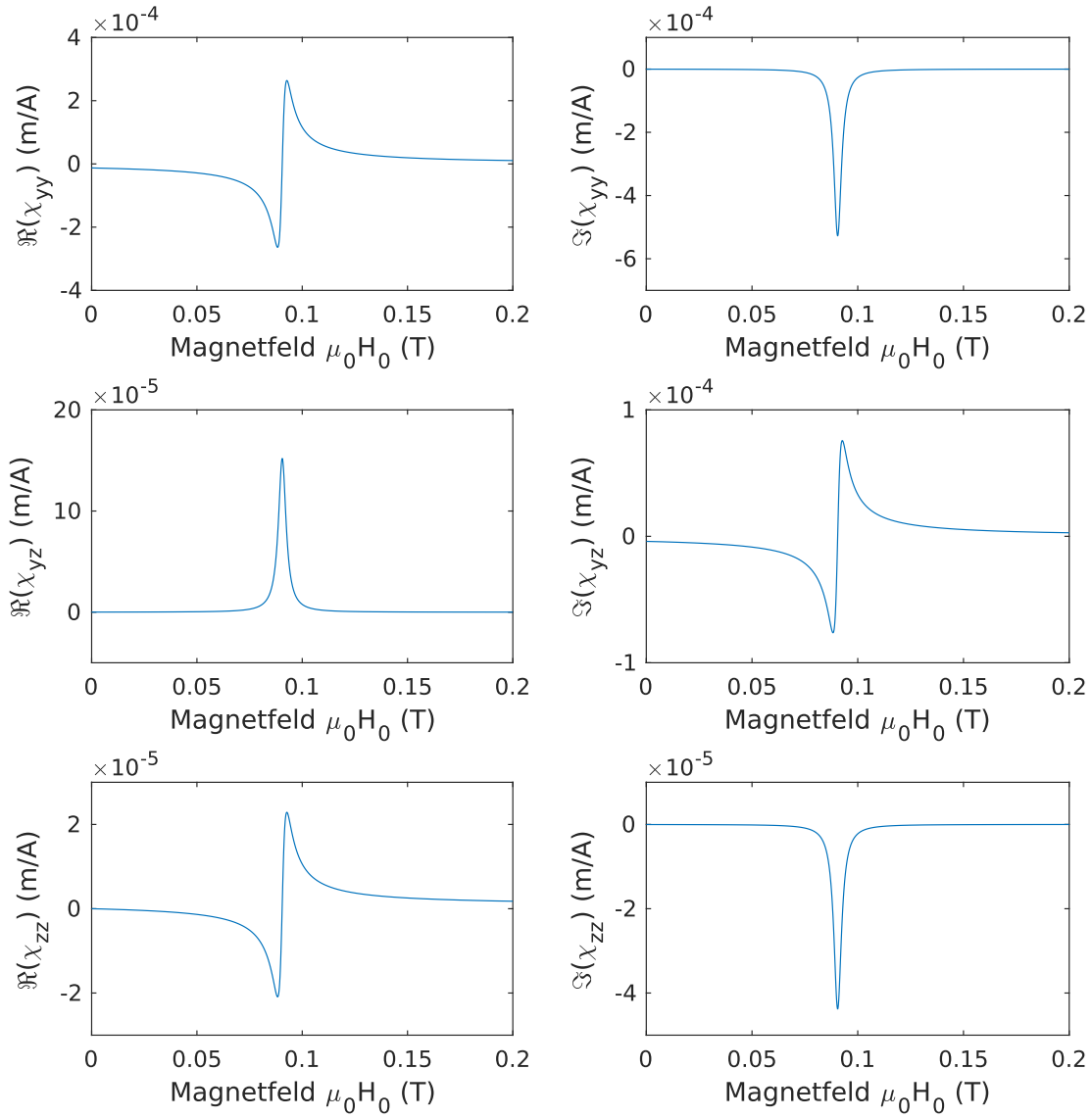

Figure 4: Line shape of real and imaginary part of susceptibilities. For the mapping, $\omega = 2\pi$ 10 GHz, $\gamma = 200\ \frac{\mathrm{GHz}}{\mathrm{T}}$, $\mu_0 M_S = 1$ T, and $\alpha = 0.007$ are used. The real parts of χ_{yy} and χ_{zz} have the form of an antisymmetric Lorentz curve and the imaginary parts are symmetric Lorentz curves. For χ_{yz} the opposite is true

.

2.5 Ferromagnetic resonance - damping

The dependence of linewidth on microwave frequency ω in ferromagnetic resonance measurements is described by the following empirical equation [10, 12]:

$$\mu_0 \Delta H = \mu_0 \Delta H(0) + \frac{\alpha \omega}{\gamma} \tag{45}$$

The $\frac{\alpha\omega}{\gamma}$ part of the damping is thereby generated by intrinsic mechanisms and can already be accounted for in the LLG by the Gilbert damping parameter α. It is mainly caused by Eddy currents (Foucault's currents), direct magnon-phonon scattering, or relaxation via itinerant electrons [10, 12]. The offset $\Delta H(0)$ comes from extrinsic mechanisms and is caused by defects or inhomogeneities in the sample [10].

3 Experimental basics and evaluation

3.1 General structure of an FMR-spectrometer

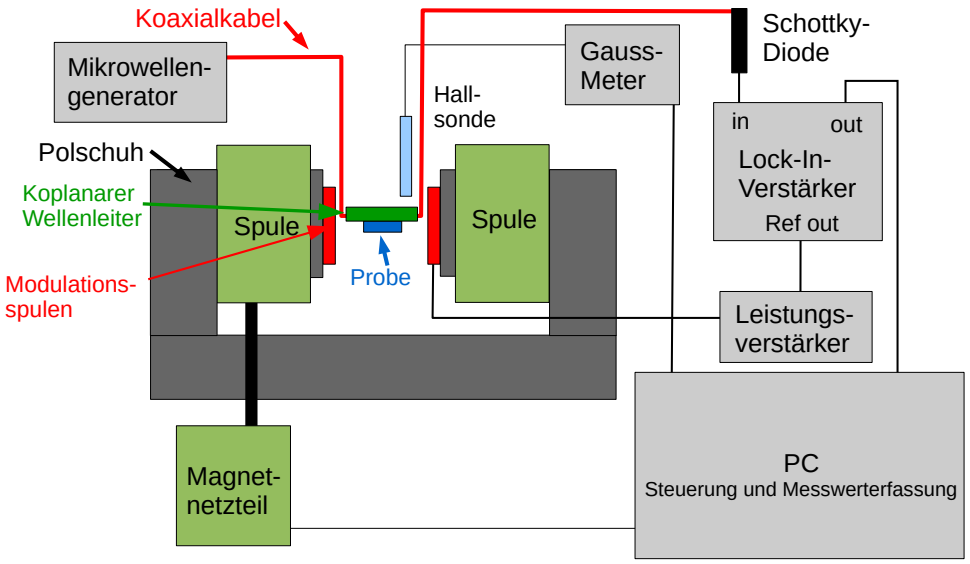

Figure 5: Construction of the FMR spectrometer used in experiment. A frequency generator produces microwaves, which are guided via coaxial cables through the waveguide and finally to the Schottky diode. On the waveguide, the sample is in the field of an electromagnet and a small modulation coil. The intensity of the microwaves is detected by a Schottky diode and measured by a lock-in amplifier. Fig. after [6]

In this experiment, a simple FMR spectrometer is available to understand the basic principles of ferromagnetic resonance. The following description of an FMR spectrometer follows [6] in essential parts.

In FMR measurements, the magnetic moments in the sample are excited to precess around the effective magnetic field by an irradiated high-frequency magnetic field $\vec{h}$ in the microwave range [10, 12]. The sample is thereby in the constant magnetic field $\vec{H}_0$ of an electromagnet. At a certain frequency and magnetic field strength $\vec{H}_{\mathrm{FMR}}$ resonance occurs and the absorption of microwaves becomes maximum [10, 12, 14]. To measure the resonance of the sample, the experiment varies the magnetic field at constant microwave frequency and simultaneously measures the absorption of microwaves in the sample using a Schottky diode.

The sample is located between the pole pieces of an electromagnet on a waveguide so that the sample is approximately centered and level on the waveguide. The block diagram shown in Figure **??** can be used to illustrate the setup. The power supply of the magnet generates a coil current of up to 20 A, which causes a magnetic field of approximately 490 mT between the pole pieces of the magnet.

To measure the field strength, a Hall probe is placed as centrally as possible between the pole pieces. The Hall probe was calibrated in advance of the experiment using a DPHH (2,2-diphenyl-1-picrylhydrazyl) sample. In this complex organic molecule, exactly one unpaired electron occurs, so its g-factor is approximately that of a free electron. Using the known g-factor, the resonant field strength can be calculated at a fixed microwave frequency, and the experimentally measured field strength can be matched with the calculated one. A Gaussmeter measures the values for the field strength and transmits them to the measurement program on the PC. During the measurement, the magnetic field is increased linearly with time by the measurement program.

Exercise 10: Find out how magnetic field measurement with a Hall sensor works. Why is calibration necessary to determine the exact magnetic field at the sample position?

A microwave field is required to excite the precession of the magnetization. In the FMR setup used, the microwaves are generated by a microwave generator that allows both the power and the frequency to be varied over a wide range. Frequencies from 2 to 26 GHz and microwave powers up to 13 dBm can be generated. The microwaves are transported via coaxial cables from the microwave generator to the coplanar waveguide. The sample is placed on the waveguide and is therefore in its magnetic field. The sample absorbs part of the irradiated power. The intensity of the remaining microwave radiation is measured using a Schottky diode.

Since the transmitted power changes only slightly due to microwave absorption in the sample, the change in diode voltage is measured with a lock-in amplifier. For measurements with a lock-in amplifier, the measurement signal must be modulated with a reference signal. For this purpose, a sinusoidal reference signal with the frequency 620 Hz is generated with a frequency generator, which is already integrated in the lock-in amplifier in the setup considered here. Care must be taken to select a frequency that is not a multiple of the mains frequency of 50 Hz. The reference signal is amplified by a power amplifier and applied to the modulation coils. This results in a small modulation of the external magnetic field $\vec{H}_0$. The lock-in amplifier now filters out from the measurement signal the component with the same frequency and a defined phase relationship with respect to the reference signal, which significantly improves the signal-to-noise ratio.

Exercise 11: Find out about the operation and internal structure of a lock-in amplifier. Make a block diagram of a lock-in amplifier. Also find out about the different types of noise and their frequency spectrum. For example, you can use the following application note from Stanford Research Systems for this purpose
http://www.thinksrs.com/downloads/PDFs/ApplicationNotes/AboutLIAs.pdf

3.2 Microwave technology

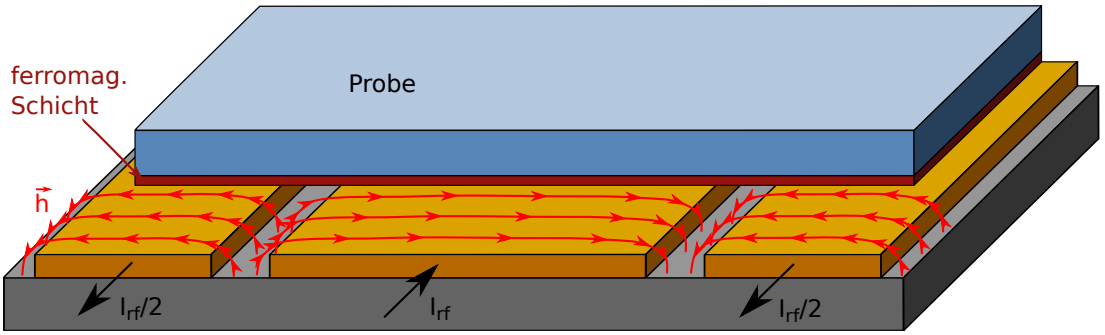

Figure 6: Principle of a coplanar waveguide. The coplanar waveguide consists of three parallel conductive paths through which a high-frequency current flows. This results in the microwave excitation field $\vec{h}$ around the traces, which is outlined by the red field lines. The sample is placed on the waveguide with the ferromagnetic layer facing downwards, so that its magnetic moments can be excited to precession by $\vec{h}$.

Here, the microwave components used in the experiment will be briefly explained. In the FMR experiments performed here, the sample is placed on a coplanar waveguide. A coplanar waveguide is a device consisting of three parallel metallic conductors [10]. In figure 6 such a waveguide is shown schematically. The middle of the traces is the signal line on which the microwave power is transported [10]. The two outer lines are ground lines [10]. The magnetic field direction in the vicinity of a coplanar waveguide can be easily determined by the right-hand rule. This results in the field directions shown in figure 6. Since the sample covers the complete waveguide, the microwave magnetic field will be under different directions with respect to the sample. Here, the excitation field points perpendicular between the waveguides and parallel to the sample plane on the waveguides. Thus, for a microwave field parallel to the equilibrium position of the magnetization, no precession of the magnetization is excited in the x-direction in the coordinate system xyz (the dynamic magnetization components $\mathfrak{m}_y$ and $\mathfrak{m}_z$ are independent of h_x), the direction of the signal line of the waveguide should be parallel to the external field so that its alternating field points perpendicular to the field direction and equilibrium magnetization.

The intensity of the microwaves is measured with a Schottky diode. This is a special form of semiconductor diode that works with a metal-semiconductor contact.

Exercise 12: Inform yourself about the phenomenological functioning of a diode. What is the voltage drop across a diode when it is connected in series with a resistor to an AC voltage source? Find out about the special characteristics of a

Schottky diode compared to other semiconductor diodes. The physical operation of a diode (band diagrams) don‘t need be understood .

3.3 Evaluation of the resonance spectra

To record an FMR spectrum, at constant microwave frequency ω the external DC magnetic field $\vec{H}_0$ is slowly increased and in parallel the absorption of microwaves is measured via the Schottky diode voltage. The absorption of microwaves during the ferromagnetic resonance of the sample is described by the imaginary part of the susceptibility χ_{yy}, which has the form of a symmetric Lorentz curve [10, 12, 14]. However, the total absorption is proportional to an asymmetric Lorentz curve because, in addition to the symmetric line shape of the absorption, there is a dispersive component which, like the real part of χ_{yy}, has an antisymmetric line shape.

The measurement of the FMR spectra is performed with the help of a lock-in amplifier. This does not measure the absorption itself, but the change of the absorption with the external DC magnetic field H_0. Therefore, the measured curves correspond to the derivative of the absorption with respect to the field H_0. Introducing the FMR amplitude A, the fit function $f(H_0)$ for the FMR spectra can now be defined.

$$\begin{aligned} f(H_0) &\propto \frac{\mathrm{d}}{\mathrm{d}H_0}\Big(\Im(\chi_{yy})\cos\epsilon + \Re(\chi_{yy})\sin\epsilon\Big) \\ &= A\left(-\frac{2\Delta H^3(H_0 - H_{\mathrm{FMR}})\cos\epsilon}{\Big((H_0 - H_{\mathrm{FMR}})^2 + \Delta H^2\Big)^2} + \frac{\Delta H^2(\Delta H^2 - (H_0 - H_{\mathrm{FMR}})^2)\sin\epsilon}{\Big((H_0 - H_{\mathrm{FMR}})^2 + \Delta H^2\Big)^2}\right) \end{aligned} \tag{46}$$

In addition to the last equation, an offset and a slope must be considered when fitting the curves [14]. In the following figure 7 a typical FMR spectrum fitted with equation (46) is shown. The two most important quantities that can be determined from the fit curve are the resonant field strength H_{FMR} and the linewidth δH [10, 12]. To perform the experiment, a fit program is provided to determine the resonant field H_{FMR} and the linewidth ΔH.

For nearly antisymmetric FMR spectra, the resonance field strength and linewidth can also be read directly from the measured spectra (see Fig. 7). The field at which the spectrum intercepts th field axis indicated the value of the resonance field H_{FMR}. The line width is proportional to the distance ΔH^{pp} between the two extrems, so that $\Delta H = \sqrt{3}/2\ \Delta H^{pp}$ [10, 12, 14].

4 Available samples

- puttered permalloy film (an alloy with composition $\mathrm{Ni_{81}Fe_{19}}$) with a film thickness of 50 nm protected against oxidation with a gold layer.

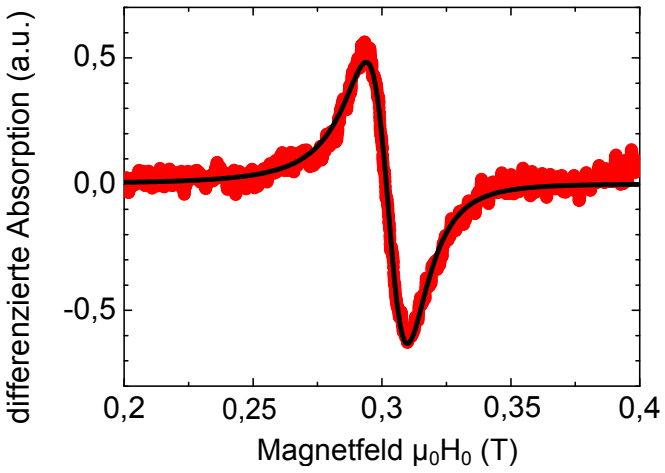

Figure 7: The figure shows a typical FMR spectrum. The points drawn in red represent the recorded measured values, the black line shows the fit according to equation (46). Using the fit, the resonant field strength $\mu_0 H_{\mathrm{FMR}} = 303.2$ mT and the linewidth $\mu_0 \delta H = 13.8$ mT can be determined. The figure shows a typical FMR spectrum. The points drawn in red represent the recorded measured values, the black line shows the fit according to equation (46). Using the fit, the resonant field strength $\mu_0 H_{\mathrm{FMR}} = 303.2$ mT and the linewidth $\mu_0 \delta H = 13.8$ mT can be determined. Fig. from[6].

- An yttrium iron garnet (YIG) layer of about 20 nm thickness grown by sputter deposition on gadolinium gallium garnet.

5 Experimental procedure

5.1 Influence of the measurement parameters

- Insert the specimen holder for the in-plane configuration, on which the permalloy specimen is already glued, into the setup.
- Set a frequency of 10 GHz and a power of 0 dBm on the microwave generator. Record a spectrum with a modulation current of 5 mA, a time constant of 0.1 s, and a sweep speed of 1 $\frac{\mathrm{mT}}{\mathrm{s}}$. Use this correctly recorded spectrum as a reference below.
- Vary the modulation current strength up and down starting from the value given in the previous point and observe the effect on the spectrum. Determine the line width for each spectrum. Record at least five curves with current strengths ranging from 0.5 mA to 200 mA. Change the sensitivity of the lock-in amplifier in case the signal is too small or cut off.

- Set the values mentioned at the beginning again. Then vary the time constant at the lock-in amplifier up and down starting from the value mentioned at the beginning and observe the influence on the spectrum. Determine the line width for each spectrum. Record at least four curves with time constants ranging from 1 ms to 10 s.

- Set the values given at the beginning. In the following, vary the sweep speed up and down starting from the value mentioned in the previous point and observe the effect on the spectrum. Determine the line width for each spectrum. Record at least five curves with velocities from 0.1 $\frac{\mathrm{mT}}{\mathrm{s}}$ to 50 $\frac{\mathrm{mT}}{\mathrm{s}}$.

5.2 Frequency dependence in the in-plane configuration on permalloy

- Again, set reasonable parameters for modulation field, sweep velocity and time constant. Now change the microwave frequency in the range from 2 to 20 GHz and follow the resonance line of Permalloy. You can do this by confining the magnetic field to the range where the resonance is expected to occur to save time.

- Evaluate the measured resonance lines in terms of resonance field strength and line width using the fit program.

- Interpret the resonance fields using the Kittel formula in equation (36). Use it to determine $\mu_0 M_{\mathrm{eff}}$. Critically analyze your fit results and try to find reasons for deviations from the expected values. Note that the g-factor of electrons in permalloy is about 2.14 (corresponding to $\gamma = 188\ \frac{\mathrm{GHz}}{\mathrm{T}}$) [12].

- Interpret the line widths using equation (45). Determine the intercept of the line width and the Gilbert "damping" parameter α.

5.3 Examination of an ytrium-iron-garnet sample

5.3.1 In-plane configuration

- Now place the YIG specimen on the in-plane specimen holder instead of the permalloy specimen.

- At a microwave frequency of 2 GHz, try to record an initial spectrum. Use a magnetic field range of 15 to 35 mT. Use a low sweep speed of 0.3 $\frac{\mathrm{mT}}{\mathrm{s}}$ due to the expected low linewidths, and reduce the modulation current to 3 mA and the time constant to 30 ms.

- Based on this spectrum, consider reasonable measurement parameters for the following spectra. Consult with the supervisor if you are unsure of your choice.

- In the following, vary the microwave frequency from 2 to 11 GHz and determine resonance field and linewidth for each spectrum. Record ten spectra. For each spectrum, determine the resonance position by reading and approximately averaging over all peaks present.

- Interpret the results by finding the resonance field using equation (36) and the linewidth using equation (45). Determine the effective magnetization $\mu_0 M_{\text{eff}}$ of the YIG sample. Use the literature value $g \approx 2.01$ for YIG ($\gamma \approx 177 \frac{\text{GHz}}{\text{T}}$) [15].

5.3.2 Perpendicular configuration

- Here, the same specimen is to be measured again in the vertical configuration. To do this, insert the specimen holder for the vertical configuration, equipped with an identical specimen, into the setup.

- First, try to record a spectrum at a frequency of 2 GHz. Use the same parameters as for the in-plane configuration.

- Vary the microwave frequency from 2 GHz to 8 GHz and determine the resonant field approximately as described in the previous section. Record ten spectra.

- Interpret the results for the resonant field using equation (37) and determine the effective magnetization $\mu_0 M_{\text{eff}}$ and the gyromagnetic ratio γ. Compare the result with the measurements in the in-plane configuration.

6 Protocol requirements

The protocol should include the following aspects:

- Magnetic energies in the ferromagnet

- Theory of ferromagnetic resonance. Start from the LLG and cover the essential aspects of the theory. Skip complex derivations (e.g., coordinate transformations in the effective field, derivation of the line shape). Derive the resonance conditions.

- Describe the FMR experiment and the equipment used in the experiment.

- Description of the performed measurements
  - Influence of the measurement parameters. Discuss the influence of the different measurement parameters on the line width of the resonance. Try to establish criteria to find the optimal measurement parameters.

- Frequency dependence on a permalloy sample. Evaluate the recorded spectra in terms of linewidth and resonance field strength and determine the material parameters of permalloy.
- Measurements on YIG sample. Evaluate the spectra in terms of resonance field strength by manual averaging over all peaks and determine the effective magnetization. Compare the measurements in the in-plane and perpendicular configurations.

7 Further literature

- M. Härtinger, Untersuchung magnetischer Materialien mit Methoden der Ferromagnetischen Resonanz, Dissertation, Universität Regensburg, 2016, verfügbar online unter https://epub.uni-regensburg.de/35434/1/Thesis.pdf
- G. Woltersdorf, Spin-Pumping and Two-Magnon Scattering in Magnetic Multilayers, Dissertation, Simon Fraser University, 2004, verfügbar online unter https://epub.uni-regensburg.de/14960/1/Woltersdorf-PhD04.pdf
- S. Blundell, Magnetism in Condensed Matter
- J. M. D. Coey, Magnetism and magnetic materials
- C. P. Slichter, Principles of Magnetic Resonance

References

[1] J.H.E. Griffiths. Anomalous High-frequency Resistance of Ferromagnetic Metals. *Nature*, 158:670–671, November 1946.

[2] E. Zavoisky. Spin Magnetic Resonance in The Decimetre-Wave Region. *J. Phys. USSR*, 10:197, November 1946.

[3] C. Kittel. On the Theory of Ferromagnetic Resonance Absorption. *Phys. Rev.*, 73:155–161, Jan 1948.

[4] L.D. Landau und E. Lifshitz. On the theory of the dispersion of magnetic permeability in ferromagnetic bodies. *Phys. Z. Sowjetunion*, 8:153–169, 1935.

[5] T.L. Gilbert. A Lagrangian formulation of the gyromagnetic equation of the magnetization field. *Phys. Rev.*, 100:1243–1244, 1955.

[6] T.N.G. Meier. Temperaturabhängige Messungen des inversen Spin-Hall-Effekts. Bachelorarbeit, Universität Regensburg, Fakultät Physik, Oktober 2012.

[7] T.N.G. Meier. Thermodynamical properties of fluctuating magnetic stripe domains in ultrathin Fe/Ni/Cu(001) and Ni/Fe/Cu(001) films. Masterarbeit, Universität Regensburg, Fakultät Physik, Dezember 2014.

[8] J.M.D. Coey. *Magnetism and Magnetic Materials*. Cambridge University Press, 2009.

[9] S. Blundell. *Magnetism in Condensed Matter*. Oxford University Press, 2001.

[10] M.O. Härtinger. Magnetische Eigenschaften neuer ferromagnetischer Maerialien. Masterarbeit, Universität Regensburg, Fakultät Physik, August 2011.

[11] J. A. Osborn. Demagnetizing Factors of the General Ellipsoid. *Phys. Rev.*, 67:351–357, Jun 1945.

[12] G. Woltersdorf. *Spin-Pumping and Two-Magnon-Scattering in Magnetic Multilayers*. Dissertation, Simon Fraser University, Department of Physics, August 2004.

[13] M.O. Härtinger. *Untersuchung magnetischer Materialien mit Methoden der Ferromagnetischen Resonanz*. Dissertation, Universität Regensburg, Fakultät für Physik, März 2016.

[14] Z. Celinski, K.B. Urquhart, und B. Heinrich. Using ferromagnetic resonance to measure the magnetic moments of ultrathin films. *Journal of Magnetism and Magnetic Materials*, 166(1):6 – 26, 1997.

[15] Seongjae Lee, Scott Grudichak, Joseph Sklenar, C. C. Tsai, Moongyu Jang, Qinghui Yang, Huaiwu Zhang, und John B. Ketterson. Ferromagnetic resonance of a YIG film in the low frequency regime. *Journal of Applied Physics*, 120(3):033905, 2016.